Am J Transl Res 2019;11(1):314-326
www.ajtr.org /ISSN:1943-8141/AJTR0082401

Original Article

Downregulation of angiopoietin-like protein 2 inhibits cementoblast differentiation partially by activating the ERK1/2 signaling pathway

Chenxi Jiang[1], Huan Liu[1,2], Hualing Sun[1,2], Xiaoxuan Wang[1], Haiqing Liao[1], Li Ma[1], Zhengguo Cao[1,2]

[1]*The State Key Laboratory Breeding Base of Basic Science of Stomatology (Hubei-MOST KLOS) and Key Laboratory for Oral Biomedical Engineering of Ministry of Education (KLOBME), School and Hospital of Stomatology, Wuhan University, Wuhan, China;* [2]*Department of Periodontology, School and Hospital of Stomatology, Wuhan University, Wuhan, China*

Received July 10, 2018; Accepted December 18, 2018; Epub January 15, 2019; Published January 30, 2019

Abstract: Angiopoietin-like protein 2 (ANGPTL2) is abundantly expressed in adipose tissue, is associated with tissue homeostasis, and promotes osteoblast and chondrocyte differentiation. In teeth, cementum, a thin layer of mineralized tissue that is formed by cementoblasts, covers the entire root surface and is a vital component of periodontium. The cementoblasts regulate the deposition and mineralization of the cementum matrix. However, the effects of ANGPTL2 on cementoblast differentiation have not been studied. The objective of this study was to elucidate the role of ANGPTL2 during cementoblast differentiation and determine its underlying mechanisms. Our results showed that the expression levels of ANGPTL2 gradually increased during cementoblast differentiation. After ANGPTL2 was knocked down using short-hairpin RNA, the levels of the osteogenic markers osterix (OSX), alkaline phosphatase (ALP), bone sialoprotein (BSP), and osteocalcin (OCN) decreased. In addition, ALP activity and the number of calcified nodules were dramatically reduced compared with those in the negative control. Interestingly, the ERK1/2 signaling pathway was activated after ANGPTL2 knockdown. Treatment with PD98059, the inhibitor of the ERK1/2 signaling pathway, partially rescued the decreased differentiation capability of cementoblast caused by ANGPTL2 downregulation. Collectively, ANGPTL2 knockdown inhibited cementoblast differentiation partially by activating the ERK1/2 signaling pathway. These findings suggest that ANGPTL2 was indispensable in cementoblast differentiation.

Keywords: ANGPTL2, dental cementum, cementogenesis, ERK1/2 signaling pathway, cementoblast differentiation, periodontal reconstruction

Introduction

Human periodontitis is a highly prevalent inflammatory disease that destroys connective tissues and leads to absorption of the alveolar bone. Periodontitis is the primary cause of tooth loss [1-3]. Cementum, a thin layer of mineralized tissue formed by cementoblasts, encases the entire surface of the root dentin and supports the periodontal ligament fibers between the tooth and surrounding alveolar bone [4, 5]. Therefore, the formation of new cementum is essential and critical for successful periodontal reconstruction [6, 7]. Cementoblasts are responsible for the deposition and mineralization of the cementum matrix. The cells have numerous characteristics similar to those of osteoblasts, such as the expression of osterix (OSX), alkaline phosphatase (ALP), bone sialoprotein (BSP), and osteocalcin (OCN), and have the capacity to produce calcified nodules *in vitro* [8-12]. Therefore, exploring the key molecules and underlying mechanisms that regulate cementoblast differentiation is essential for cementum regeneration and periodontal reconstruction.

Angiopoietin-like proteins (ANGPTLs), a family of secreted proteins, contain a coiled-coil domain at the N-terminal for oligomerization and a fibrinogen-like domain at the C-terminal. Although ANGPTLs are structurally conserved in

Table 1. Primers used for qRT-PCR

Genes	Forward primer (5'-3')	Revers primer (3'-5')
Gapdh	GGAGATTGTTGCCATCAACGA	GAAGACACCAGTAGACTCCACGACA
Sp7	CCTCTCGACCCGACTGCAGATC	AGCTGCAAGCTCTCTGTAACCATGAC
Bglap	GAGGACCATCTTTCTGCTCACT	CGGAGTCTGTTCACTACCTTATTG
Bsp	GAGCCTCGTGGCGACACTTA	AATTCTGACCCTCGTAGCCTTCATA
Alp	TGTGGAATACGAACTGGATGAG	ATAGTGGGAATGCTTGTGTCTG
Angptl2	GGAGGTTGGACTGTCATCCAGAG	GCCTT GGTTCGTCAGCCAGTA

the angiopoietin protein family, they do not bind to the angiopoietin receptor Tie1 or Tie2, indicating that the roles of these proteins are distinct from those of angiopoietins [13-15]. ANGPTL2 is abundantly expressed in adipose tissues and is a key inflammatory mediator related to obesity and systemic insulin resistance [16, 17]. Additionally, ANGPTL2 is associated with chronic inflammation from several diseases such as renal fibrosis [18], rheumatoid arthritis [19], and atherosclerosis [20]. A study on periodontal disease has shown that ANGPTL2 regulated *Porphyromonas gingivalis* lipopolysaccharide-induced inflammatory cytokines in human gingival epithelial cells and that the concentration of ANGPTL2 measured in gingival crevicular fluid increased in chronic periodontitis patients [21]. Moreover, ANGPTL2 plays essential roles in cell differentiation, including that of adipocytes [17], chondrocytes [22], and osteoblasts [23]. However, the function of ANGPTL2 in cementoblast differentiation and the underlying mechanisms have not been clarified.

Here, we aimed to investigate the expression pattern and explicit role of ANGPTL2 in cementoblast differentiation and to clarify which signaling pathways are involved in the differentiation process. Our data analysis suggests that ANGPTL2 is an indispensable molecule in cementoblast differentiation.

Materials and methods

Cell culture

An immortalized mouse cementoblast cell line OCCM-30 [10] was kindly provided by Dr. Martha J. Somerman (National Institutes of Health, Bethesda, MD, USA) and was cultured as previously described [24, 25]. Briefly, the cells were cultured in Dulbecco's Modified Eagle's Medium (HyClone, USA) containing 10% fetal bovine serum (FBS; Gibco) and 1% penicillin/streptomycin and were incubated in a humidified atmosphere of 5% CO_2 at 37°C. The cells were seeded in 12-well plates at a density of 1×10^5 cells/well to induce osteogenic differentiation. At 80% confluence, the culture medium was replaced with the osteogenic induction medium (OIM) containing 5% FBS supplemented with 10 mM Naβ-glycerophosphate (Sigma-Aldrich, St. Louis, MO, USA) and 50 μg/mL ascorbic acid (Sigma-Aldrich).

Quantitative real-time PCR (qRT-PCR)

Total RNA was isolated using TRIzol reagent (Invitrogen, Santa Clara, CA, USA). First-strand cDNA was transcribed from 1 μg RNA using a HiScript® II 1st Strand cDNA Synthesis Kit (Vazyme Biotech Co., Ltd., NanJing, China). Quantitative real-time polymerase chain reaction (qRT-PCR) was conducted in triplicate on the QuantStudio 6™ (Applied Biosystems Corp., Foster City, CA, USA) using ChamQ™ SYBR® qPCR Master Mix (Vazyme). *Glyceraldehyde-3-phosphate dehydrogenase* (*GAPDH*) was determined to be the internal reference and the value of $2^{-\Delta\Delta CT}$ was used for calculating the relative fold changes. The primer sequences are presented in **Table 1**.

Western blot analysis

Total protein was collected using M-PER mammalian protein extraction reagent (Thermo Fisher Scientific, Waltham, MA, USA) containing phenylmethanesulfonyl fluoride and phosphatase inhibitors (Roche Applied Science, Penzberg, Germany). After centrifugation at 13000 × g at 4°C for 15 min, the protein in the supernatant was collected and measured using a bicinchoninic acid assay kit (Beyotime). Subsequently, 30 μg protein was loaded onto 10%-12% sodium dodecyl sulfate (SDS) polyacrylamide gel and transferred onto a polyvinylidene difluoride (PVDF) membrane (Millipore, Billerica, MA, USA). The membranes were blocked with 5% nonfat milk for 1 h at room temperature and then incubated overnight at

4°C with primary antibodies for ANGPTL2 (2 μg/mL; R&D Systems, Minneapolis, MN, USA), BSP (1:1000; Cell Signaling Technology, Danvers, MA, USA), OCN (1:500; Abcam, Cambridge, UK), OSX (1:1000; Abcam), β-catenin (1:5000; Abcam), P-ERK1/2 (1:1000; Cell Signaling Technology), total ERK1/2 (1:1000; Cell Signaling Technology), P-JNK (1:1000; Cell Signaling Technology), total JNK (1:1000; Cell Signaling Technology), P-P38 (1:1000; Cell Signaling Technology), total P38 (1:1000; Cell Signaling Technology), and β-actin (1:15000; Proteintech), followed by horseradish peroxidase-conjugated secondary antibodies (1:10000; Proteintech) for 1 h at room temperature. The membranes were visualized using an enhanced chemiluminescence (ECL) kit (Advansta Inc., Menlo Park, CA, USA) and detected using X-ray films or the Odyssey LI-CDR scanner (BD Biosciences, San Jose, CA, USA). The protein density was calculated using Image J software.

Immunofluorescence staining

ANGPTL2 expression was examined using an immunofluorescence assay. OCCM-30 cells were fixed with 4% paraformaldehyde for 15 min and treated with 0.5% Triton X-100 for 15 min for permeabilization. The cells were then incubated in 10% normal goat serum at 37°C for 60 min and with primary antibodies against ANGPTL2 (1:50; Proteintech) at 4°C overnight, followed by goat anti-rabbit secondary antibody conjugated to fluorescein isothiocyanate (1:150; ZSGB-BIO). After washing with PBS, the coverslips were mounted using a fluorescent mounting medium with 4',6-diamidino-2-phenylindole (ZSGB-BIO). The images were observed under a fluorescence microscope and photographed.

Plasmid construction and lentivirus transduction

Short-hairpin (sh) RNA targeting the mouse ANGPTL2 named "SH-ANGPTL2" and a nontarget control shRNA named "SH-NC" were provided by Shanghai Genechem Co., Ltd. (China). The lentiviral vector was transfected into 293E cells together with pMD2.G and psPAX2. The culture supernatant was collected after 48 and 72 h and then filtrated using a 0.45 μm filter (Millipore). OCCM-30 cells were infected with lentivirus including polybrene (5 μg/mL) for 6 h, after which the complete culture medium was replaced. The transfected cells were prepared for future experiments.

Cell Counting Kit-8 cell proliferation assay

The effect of ANGPTL2 on cell proliferation was evaluated using the Cell Counting Kit (CCK)-8 assay (Dojindo Molecular Technology, Japan). The cells were seeded in 96-well plates at 4000 cells/well. The culture medium was changed to 10 μL CCK-8 reagent mixed with 90 μL complete medium at the indicated time points. The plates were then incubated at 37°C for 150 min, and the absorbance was measured at 450 nm.

Alkaline phosphatase staining and alkaline phosphatase activity assay

After osteogenic induction for 4 days, OCCM-30 cells were examined using ALP staining and assayed for ALP activity. For ALP staining, the cells were stained with nitro-blue tetrazolium and 5-bromo-4-chloro-3'-indolyphosphate (NBT/BCIP) (Beyotime) for 15 min and photographed according to the instructions. ALP activity was evaluated using a kit provided by Jiancheng (Nanjing, China), and the results were relative to the total protein concentration.

Alizarin red staining

After the OCCM-30 cells were cultured in OIM for 10 days, mineralized nodules were evaluated using Alizarin Red staining. The cells were treated with 1% Alizarin Red solution (pH 4.2) for 15 min after being fixed in 4% paraformaldehyde. The plates were photographed with a camera. After the images of nodules were obtained, the mineralized nodules were desorbed with 10% cetylpyridinium chloride, and the absorbance of the solution was read at 562 nm.

Statistical analysis

All values are expressed as the means ± standard deviation (SD). Statistical analysis was performed using SPSS 16.0 (SPSS Inc., Chicago, IL, USA). The Student's *t*-test was used to compare results between the two groups and one-way analysis of variance (ANOVA) was used to compare results among more than two groups. The *post hoc* Tukey test or *post hoc*

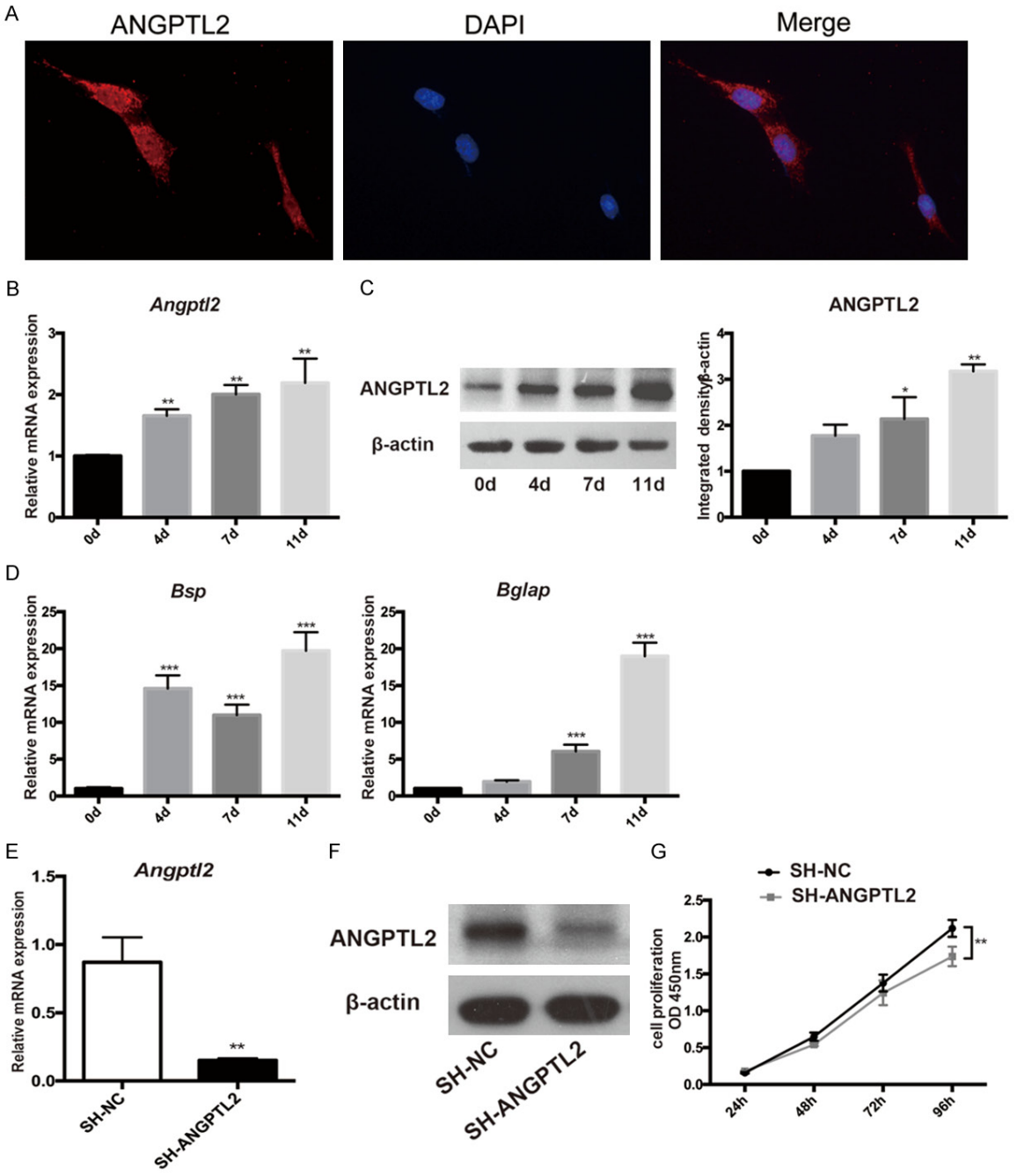

Figure 1. Immunofluorescence staining for ANGPTL2 expression and lentivirus infection of OCCM-30 cells. The effect of ANGPTL2 downregulation on cell proliferation. A. Immunofluorescence assay demonstrated that ANGPTL2 was located in the cytoplasm of OCCM-30 cells. B, C. The mRNA and protein levels of ANGPTL2 were examined by qRT-PCR and Western blotting on days 0, 4, 7, and 11. The expression level of ANGPTL2 gradually increased during osteogenic differentiation of OCCM-30 cells. The 0 day group was set as the control. *P < 0.05, **P < 0.01 (one-way ANOVA with *post hoc* Dunnett test). D. mRNA levels of osteogenic markers *Bsp* and *Bglap* were examined by qRT-PCR on days 0, 4, 7 and 11 during osteogenic differentiation of OCCM-30 cells. ***P < 0.001 (one-way ANOVA with *post hoc* Dunnett test). E, F. After infection of the cells with lentivirus and selection with puromycin (2 μg/mL) for 7 days, the mRNA and protein levels of ANGPTL2 significantly decreased in the SH-ANGPTL2 group compared with SH-NC group. **P < 0.01 (Student's *t*-test). G. Knockdown of ANGPTL2 inhibited cell proliferation as seen using the CCK-8 assay. **P < 0.01 vs SH-NC (Student's *t*-test). All data were based on three independent experiments. Values are presented as the mean ± SD.

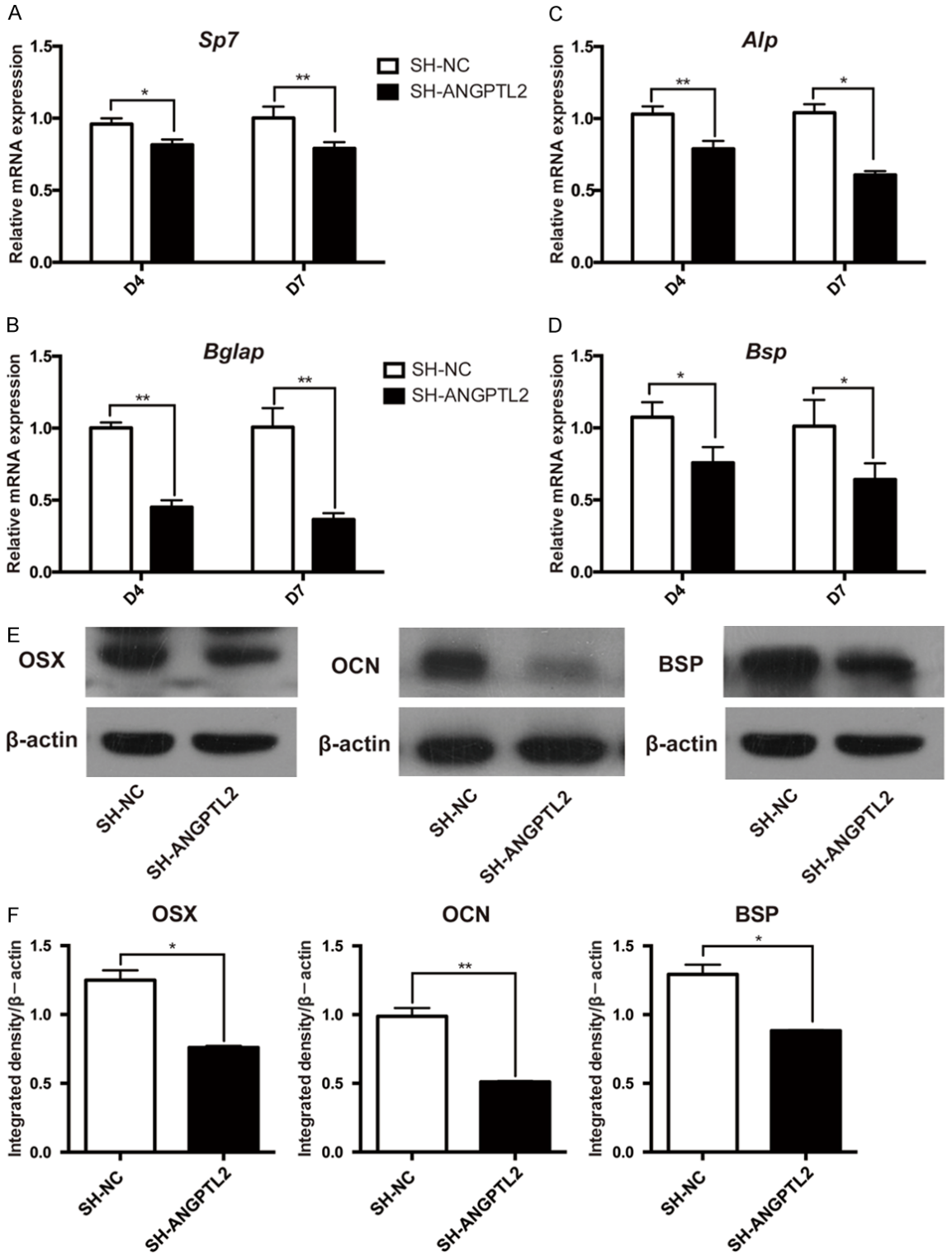

Figure 2. ANGPL2 knockdown suppressed cementoblast differentiation. A-D. mRNA levels of *Sp7*, *Alp*, *Bglap*, and *Bsp* were examined by qRT-PCR on days 4 and 7, and the expression levels in the knockdown group were lower than those in the SH-NC group during osteogenic differentiation of OCCM-30 cells. *P < 0.05, **P < 0.01 vs SH-NC (Student's *t*-test). E. The protein levels of osterix (OSX), bone sialoprotein (BSP), and osteocalcin (OCN) were detected by Western blotting on day 7 during osteogenic differentiation of OCCM-30 cells. F. Histograms representing the quantification of OSX, OCN, and BSP protein levels were obtained using Image J. *P < 0.05, **P < 0.01 vs SH-NC (Student's *t*-test). All data were based on at least three independent experiments. Values are presented as the mean ± SD.

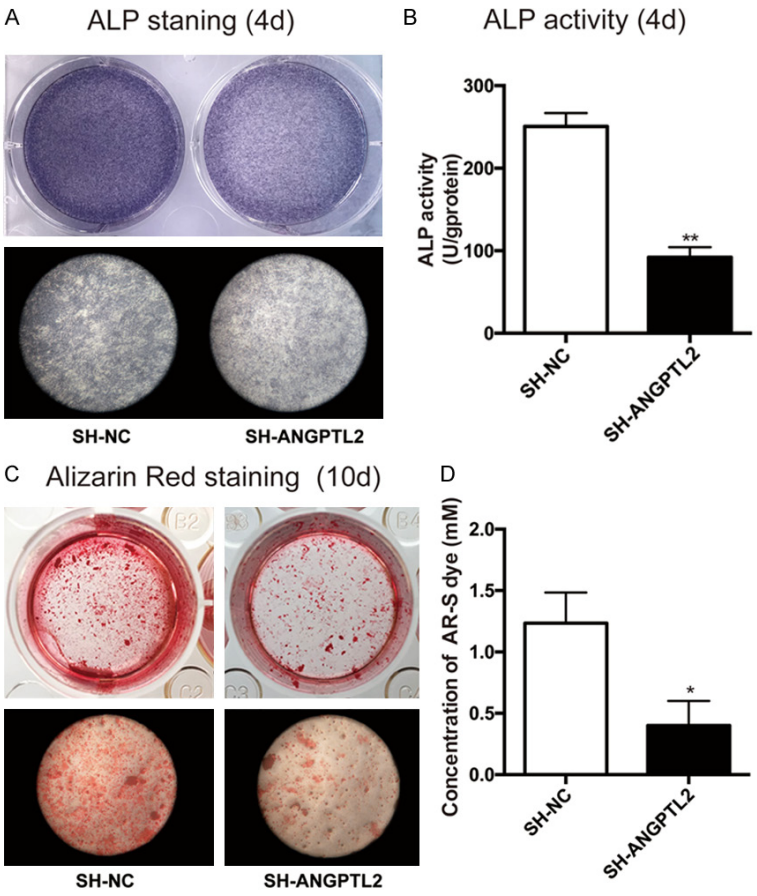

Figure 3. ANGPL2 knockdown suppressed ALP activity, ALP staining, and mineralized nodules. A. ALP staining was conducted on day 4 during osteogenic differentiation of OCCM-30 cells. The cells were stained with nitro-blue tetrazolium and 5-bromo-4-chloro-3'-indolyphosphate (NBT/BCIP) for 15 min and photographed. Additionally, the attenuated ALP staining intensity was observed in the knockdown group compared to that in the SH-NC group. B. A kit for ALP activity assay was used and the data were normalized to total protein level. Downregulation of ANGPTL2 had an evident inhibitory effect on the ALP activity of OCCM-30 cells. **P < 0.01 vs SH-NC (Student's *t*-test). C. Alizarin Red staining of the OCCM-30 cells was detected on day 10. There were fewer calcified nodules in the knockdown group than in the SH-NC group. D. Mineralized nodules were desorbed with 10% cetylpyridinium chloride, and the absorbance of the solution was read at 562 nm. *P < 0.05 vs SH-NC (Student's *t*-test). Values are presented as the mean ± SD.

Dunnett test was conducted if one-way ANOVA indicated a significant difference. All experiments were independently performed at least three times. P < 0.05 was considered statistically significant.

Results

The expression of ANGPTL2 was upregulated during cementoblast differentiation

Immunofluorescence assay demonstrated that ANGPTL2 was located in the cytoplasm of the OCCM-30 cells (**Figure 1A**). These cells were cultured in OIM for 0, 4, 7, and 11 days to investigate whether ANGPTL2 expression was influenced upon cementoblast differentiation. The increase of ANGPTL2 expression in a time-dependent manner was confirmed at mRNA and protein levels (P < 0.01, **Figure 1B**, **1C**). The expression of osteogenic gene markers *Bsp* and *Bglap* also continually increased (P < 0.001, **Figure 1D**), indicating that the cells were successfully osteogenic induced.

ANGPTL2 knockdown suppressed cementoblast differentiation

To further identify the function of ANGPTL2 during cementoblast differentiation, we silenced ANGPTL2 expression using SH-ANGPTL2 lentivirus and adopted SH-NC as the negative nontarget control. Transfection efficiency was evaluated using qRT-PCR and Western blotting (P < 0.01, **Figure 1E**, **1F**). The original western images were showed in Figure S1. A CCK-8 assay was conducted to explore the effect of ANGPTL2 on cell proliferation and showed that ANGPTL2 downregulation suppressed the proliferation of OCCM-30 cells (P < 0.01, **Figure 1G**).

After the cells were cultured in OIM for 4 and 7 days, qRT-PCR was conducted to assess the expression levels of osteogenic genes. Compared with the SH-NC group, the mRNA expression levels of *Sp7* (P < 0.05 for day 4 and P < 0.01 for day 7, **Figure 2A**), *Bglap* (P < 0.01, **Figure 2B**), *Alp* (P < 0.01 for day 4 and P < 0.05 for day 7, **Figure 2C**), and *Bsp* (P < 0.05, **Figure 2D**) were suppressed in the ANGPTL2 knockdown group. Moreover, the assessment of the protein levels using Western blotting revealed similar downward trends on day 7 (**Figure 2E**, **2F**). The original western images were showed

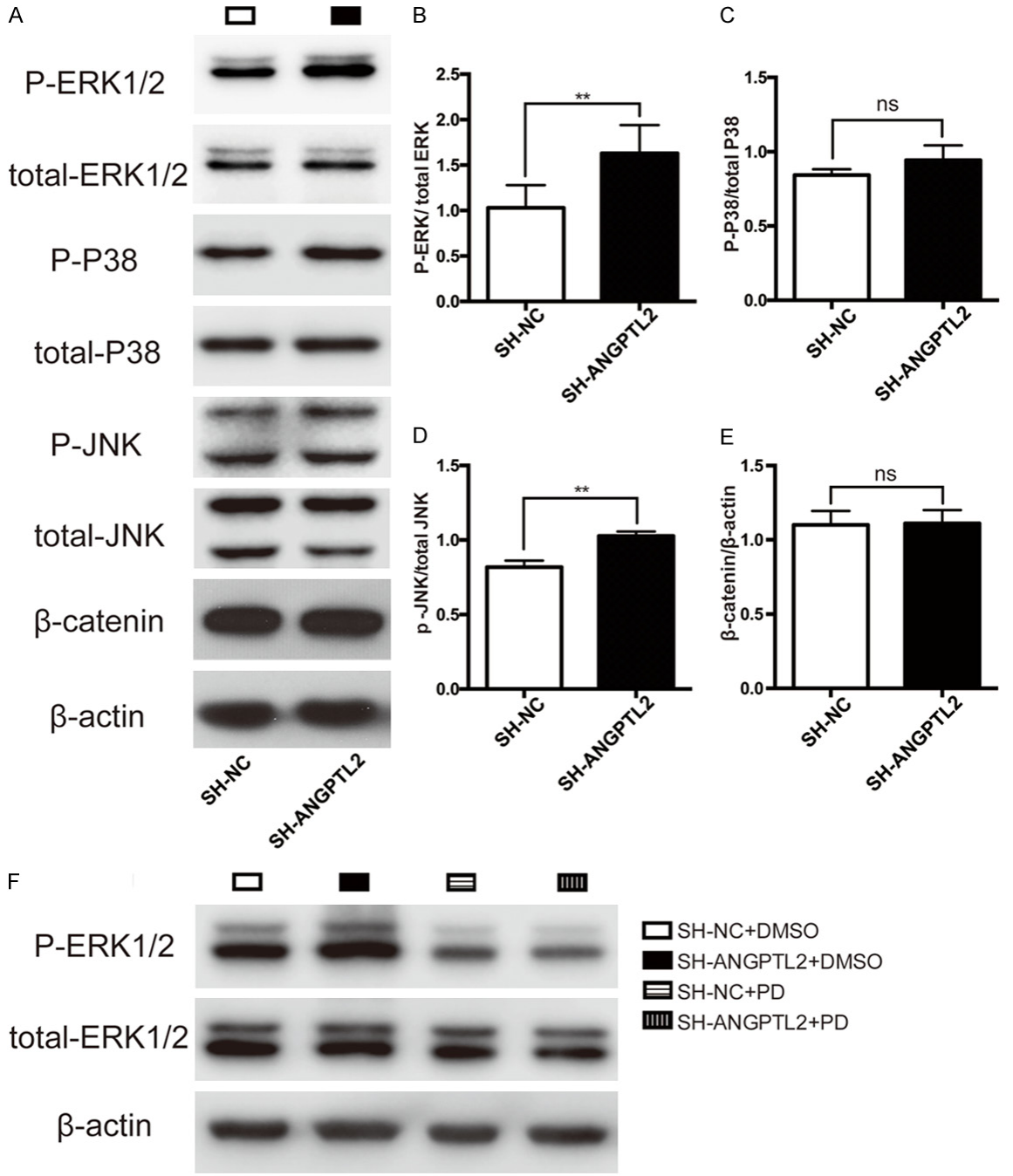

Figure 4. Activation of the MAPK signaling pathway by ANGPTL2 downregulation. A. Four different signaling pathways were detected by Western blotting-ERK1/2, P38, JNK, and β-catenin after ANGPTL2 inhibition. B-E. Histograms representing quantification of (phospho-ERK1/2)/(total ERK1/2), (phospho-P38)/(total P38), (phospho-JNK)/(total JNK), and (β-catenin)/(β-actin) ratios obtained by Image J. The results show that phospho-ERK1/2 was significantly enhanced after ANGPTL2 silencing. *P < 0.01 vs SH-NC (Student's *t*-test). F. The protein levels of (P-ERK1/2)/(total ERK1/2) significantly decreased after the cells were treated with PD98059 (10 μM) in dimethyl sulfoxide (DMSO) for 6 h compared with those treated with DMSO alone. Values are presented as the mean ± SD.

in Figure S2. Evident decreased matrix mineralization in the ANG-PTL2 knockdown group was also observed, including low ALP activity (P < 0.01, **Figure 3B**), attenuated ALP staining intensity (**Figure 3A**) and reduced mineralized nodules (P < 0.05, **Figure 3C**, **3D**). These results

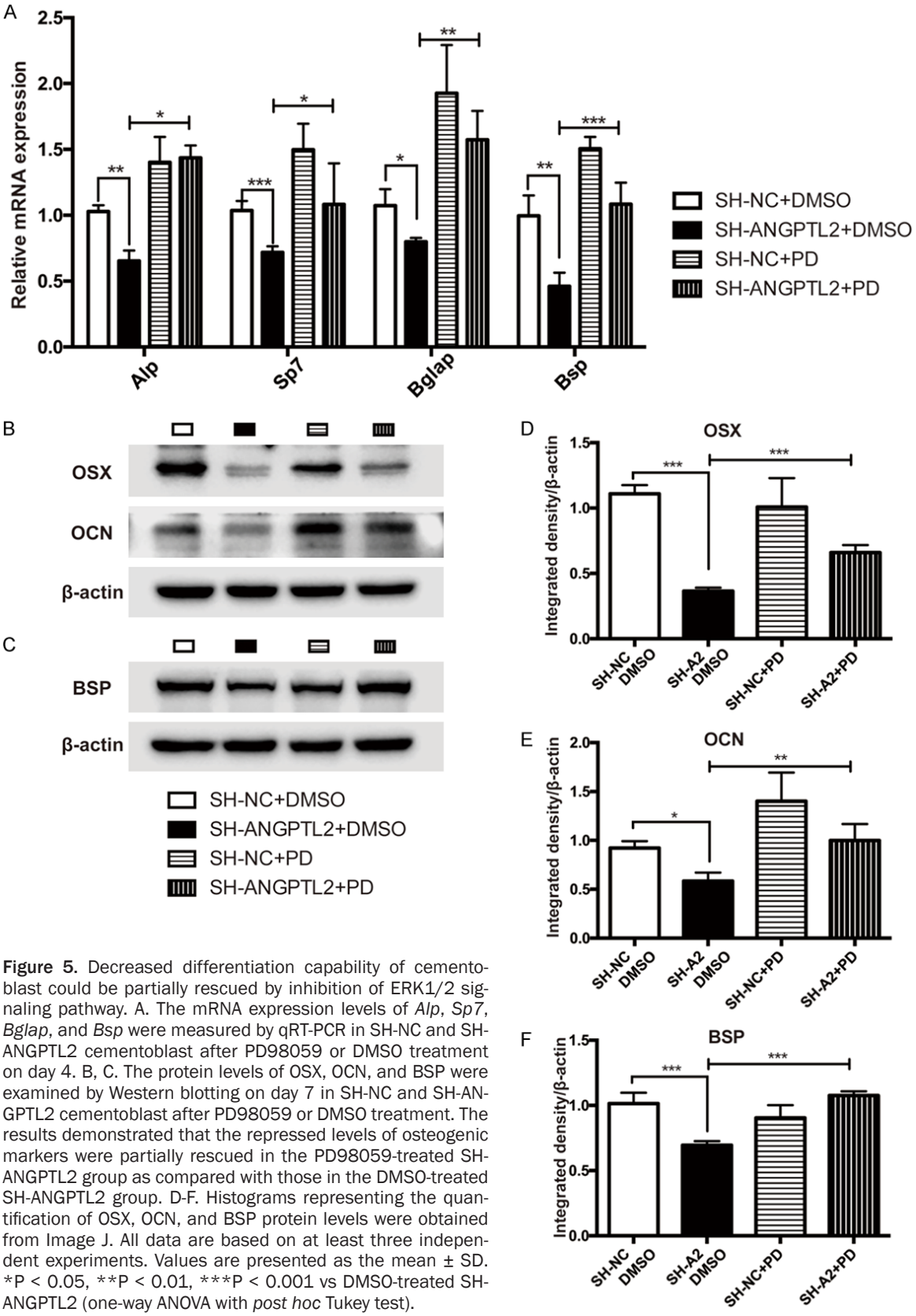

Figure 5. Decreased differentiation capability of cementoblast could be partially rescued by inhibition of ERK1/2 signaling pathway. A. The mRNA expression levels of *Alp*, *Sp7*, *Bglap*, and *Bsp* were measured by qRT-PCR in SH-NC and SH-ANGPTL2 cementoblast after PD98059 or DMSO treatment on day 4. B, C. The protein levels of OSX, OCN, and BSP were examined by Western blotting on day 7 in SH-NC and SH-ANGPTL2 cementoblast after PD98059 or DMSO treatment. The results demonstrated that the repressed levels of osteogenic markers were partially rescued in the PD98059-treated SH-ANGPTL2 group as compared with those in the DMSO-treated SH-ANGPTL2 group. D-F. Histograms representing the quantification of OSX, OCN, and BSP protein levels were obtained from Image J. All data are based on at least three independent experiments. Values are presented as the mean ± SD. *P < 0.05, **P < 0.01, ***P < 0.001 vs DMSO-treated SH-ANGPTL2 (one-way ANOVA with *post hoc* Tukey test).

demonstrated that inhibition of ANGPTL2 remarkably suppressed cementoblast differentiation.

Activation of the MAPK signaling pathway by ANGPTL2 downregulation

To further elucidate the molecular mechanisms of ANGPTL2 during cementoblast differentiation, we evaluated the effects of ANGPTL2 silencing on four different signaling pathways: ERK1/2, P38, JNK, and Wnt/β-catenin. The results of Western blotting indicated that phospho-ERK1/2 ($P < 0.01$, **Figure 4A**, **4B**) was significantly enhanced and that phospho-JNK ($P < 0.01$, **Figure 4A**, **4D**) was slightly promoted after ANGPTL2 silencing compared with those in the SH-NC group. However, the P38 (**Figure 4A**, **4C**) and Wnt/β-catenin signaling pathways (**Figure 4A**, **4E**) showed no statistical difference between the two groups. The original western images were showed in Figure S3. Therefore, the data suggested that the ERK1/2 signaling pathway was crucial during ANGPTL2-mediated cementoblast differentiation.

Decreased differentiation capability of cementoblast could be partially rescued by inhibiting the ERK1/2 signaling pathway

To further clarify the relationship between ANGPTL2 and the ERK1/2 signaling pathway, which showed the most evident change among the MAPK signaling pathways, we validated the effects of PD98059 treatment on OCCM-30 cells differentiation. The protein level of P-ERK1/2 significantly decreased after the cells were treated with 10 μM PD98059 in dimethyl sulfoxide (DMSO) for 6 hours (**Figure 4F**). Meanwhile, the repressed mRNA levels of *Alp* ($P < 0.05$, **Figure 5A**), *Bglap* ($P < 0.01$, **Figure 5A**), *Sp7* ($P < 0.05$, **Figure 5A**), and *Bsp* ($P < 0.001$, **Figure 5A**) were partially rescued in the PD98059-treated SH-ANGPTL2 group compared with those in the DMSO-treated SH-ANGPTL2 group on day 4. In addition, the results of Western blotting showed that the protein levels of OSX ($P < 0.001$, **Figure 5B**, **5D**), OCN ($P < 0.01$, **Figure 5B**, **5E**), and BSP ($P < 0.001$, **Figure 5C**, **5F**) were also recovered, which was in accordance with the results of qPCR. And the original western images were showed in Figure S4. Moreover, the results were further supported by ALP staining, ALP activity assay, and Alizarin Red staining, including high ALP activity ($P < 0.001$, **Figure 6B**), enhanced ALP staining intensity (**Figure 6A**), and increased mineralized nodules ($P < 0.001$, **Figure 6C**, **6D**) in the PD98059-treated ANGPTL2-SH group compared with those in the DMSO-treated ANGPTL2-SH group. Collectively, decreased differentiation capability of cementoblast due to ANGPTL2 downregulation could be partially rescued by inhibiting the ERK1/2 signaling pathway.

Discussion

Tooth cementum, a bone-like mineralized tissue, is an indispensable part of periodontal tissues [7]. New cementum formation is regarded as the gold standard for successful periodontal regeneration [26]. Therefore, exploring the key molecular and underlying mechanisms that regulate cementoblast differentiation is essential for cementum regeneration. ANGPTL2 plays a vital role in cell differentiation, such as that of adipocytes [17], chondrocytes [22], and osteoblasts [23]. However, the explicit function of ANGPTL2 in cementoblast differentiation and the underlying mechanisms have not been clarified. In this study, we confirmed that ANGPTL2 knockdown suppressed cementoblast differentiation partially by activating the ERK1/2 signaling pathway. This is the first study to explore the function of ANGPTL2 in periodontal tissue regeneration.

In this study, we observed that the expression of ANGPTL2 gradually increased during cementoblast differentiation, the result of which was similar to that during adipocyte differentiation [17]. However, ANGPTL2 gradually decreased during osteoblast and chondrocyte differentiation, indicating that ANGPTL2 may play a vital role in cell differentiation. After the shRNA lentivirus was used to knockdown ANGPTL2 expression, the mRNA and protein levels of osteogenic markers, ALP activity, and mineralized nodules significantly decreased. These results were in accordance with those of osteoblast and chondrocyte differentiation. Inhibition of ANGPTL2 using siRNA markedly inhibited the expression levels of ALP and OSX in MC3T3-E1 and primary osteoblasts [23]. We had previously reported that OSX was indispensable and critical for the formation of new cellular cementum [9]. In addition, ANGPTL2 contributed to chondrocyte differentiation, and ANGPTL2 knockout mice showed slower long bone growth

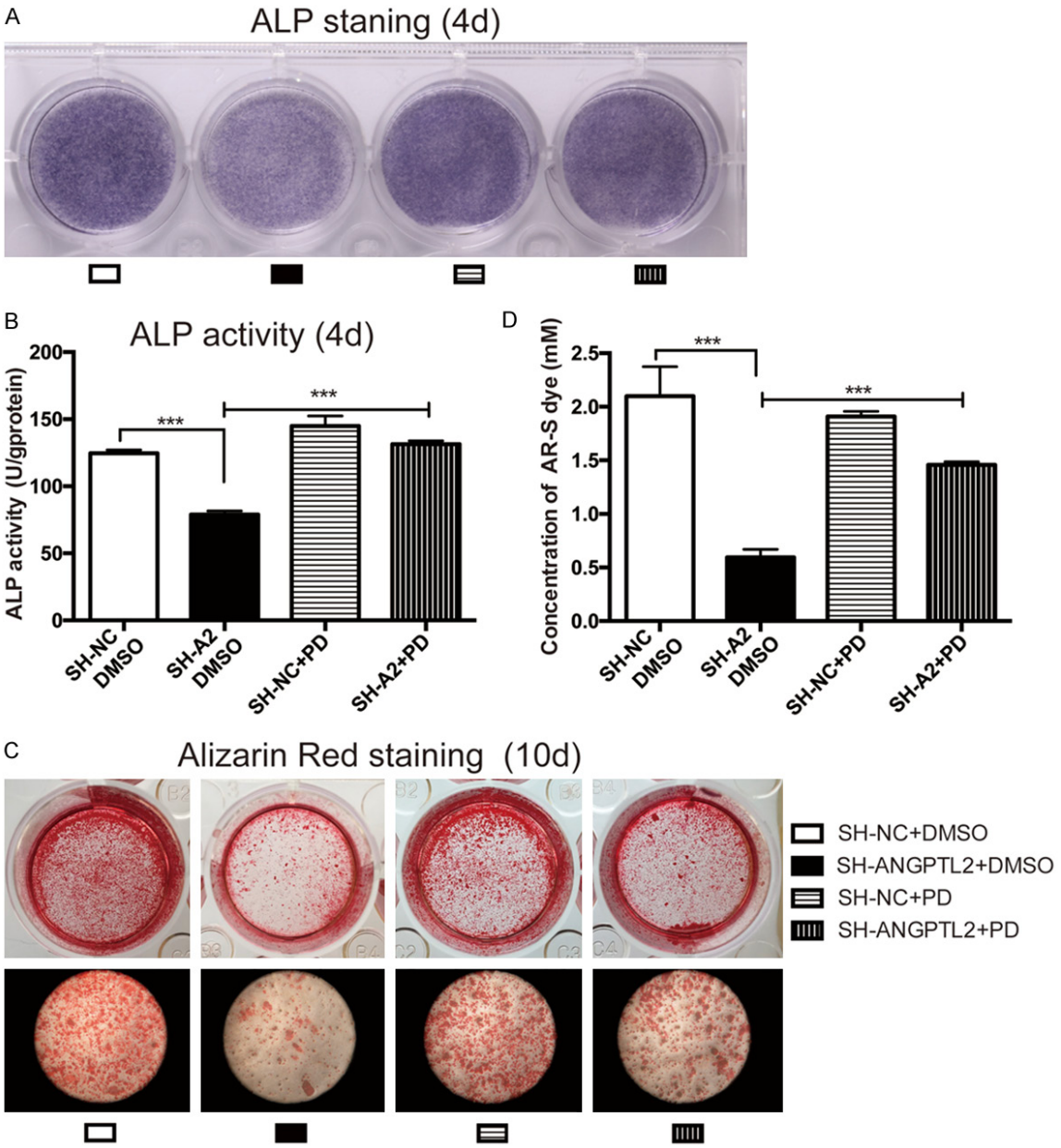

Figure 6. Decreased ALP activity and mineralized nodules could be partially rescued by inhibiting the ERK1/2 signaling pathway. A. SH-NC and SH-ANGPTL2 cementoblast were stained with ALP after PD98059 or DMSO treatment on day 4. The cells were stained with NBT/BCIP for 15 min and photographed. B. ALP activity was measured in SH-NC and SH-ANGPTL2 cementoblast after PD98059 or DMSO treatment on day 4. The results were normalized to total protein levels. The ALP activity increased after inhibiting the ERK1/2 signaling pathway using PD98059. C. Four groups were stained with Alizarin Red on day 10, and there were more calcified nodules in the PD98059-treated ANGPTL2-SH group than in the DMSO-treated ANGPTL2-SH group. D. Mineralized nodules in the four groups were desorbed with 10% cetylpyridinium chloride, respectively, and absorbance of the solution was read at 562 nm. All data were based on at least three independent experiments. Values are presented as the mean ± SD. ***P < 0.001 vs DMSO-treated SH-ANGPTL2 (one-way ANOVA with *post hoc* Tukey test).

from neonatal to adult stages because of weakened chondrocyte differentiation [22]. Although the expression pattern of ANGPTL2 varies in different cell types, the effects of ANGPTL2 on cell differentiation are similar.

Previous studies have confirmed that ANGPTL2 could regulate metastasis of osteosarcoma cells, proliferation and invasion of glia cells, inflammatory responses of peritoneal cells, and chondrocyte differentiation through MAPK

signaling pathways [27-29]. ANGPTL2 has also been reported to control epithelial regeneration and homeostasis through the BMP and WNT/β-catenin signaling pathways [30]. Here we examined whether these pathways were activated by ANGPTL2 inhibition in OCCM-30 cells. The results showed that ERK1/2 signaling pathway was significantly enhanced after ANGPTL2 inhibition. The ERK1/2 cascade plays important roles in osteogenic induction of various cell types, but the exact function is controversial. For example, ERK1/2 inhibition enhances early osteoblastic cells and C2Cl2 pluripotent mesenchymal cell differentiation and mineralization [31]. However, ERK1/2 inhibition suppresses the osteogenic differentiation of human adipose-derived and dental pulp stem cells [32, 33]. In this study, the expression levels of osteogenic markers, ALP activity, and the number of calcified nodules were enhanced after inhibiting ERK1/2 using PD98059. The results indicated that ERK1/2 inhibition could rescue the decreased differentiation capability of cementoblast due to ANGPTL2 knockdown. Similarly, the data were consistent with those of a previous report which showed that ERK1/2 inhibition promoted cementoblast differentiation [34].

The results of our study indicated that the expression level of ANGPTL2 gradually increased during cementoblast differentiation. However, whether the transcription factors or upstream molecules regulated ANGPTL2 expression remained unknown. Our previous studies have indicated that microRNA-155-3p and microRNA-3064-3p regulated cementoblast differentiation through KCTD1 and DKK1, respectively [24, 35]. Some studies have demonstrated that microRNA-25 and microRNA-221 bond directly to the 3'-untranslated region of *Angptl2* to influence the growth and migration of tumor cells [36, 37]. Therefore, further research is required to determine the regulatory mechanism of ANGPTL2-related microRNA in cementoblast differentiation

In conclusion, this study illustrated the expression pattern of ANGPTL2 during cementoblast differentiation. After ANGPTL2 was downregulated using shRNA, the expression levels of osteogenic markers, ALP activity, and the number of calcified nodules dramatically decreased compared with those in the negative control. Moreover, we confirmed that PD98059 treatment partially rescued the decreased differentiation capability of cementoblast that was caused by ANGPTL2 downregulation. In summary, our data clarified that ANGPTL2 downregulation suppressed cementoblast differentiation partially by activating the ERK1/2 signaling pathway. Moreover, our study suggested that ANGPTL2 was a molecule that was indispensable for cementum reconstruction and periodontal tissue regeneration.

Acknowledgements

This work was supported by the National Natural Science Foundation of China (81570946, 81870776), Youth Chenguang Project of Science and Technology of Wuhan City (20140-72704011255), Natural Science Foundation of Hubei Province (2015CFB259).

Disclosure of conflict of interest

None.

Address correspondence to: Zhengguo Cao, Department of Periodontology, School and Hospital of Stomatology, Wuhan University, 237 Luoyu Road, Hongshan District, Wuhan 430079, China. Tel: +86-27-87686212; E-mail: caozhengguo@whu.edu.cn

References

[1] Kassebaum NJ, Bernabe E, Dahiya M, Bhandari B, Murray CJ and Marcenes W. Global burden of severe periodontitis in 1990-2010: a systematic review and meta-regression. J Dent Res 2014; 93: 1045-1053.

[2] Yang H, Xiao L, Zhang L, Deepal S, Ye G and Zhang X. Epidemic trend of periodontal disease in elderly Chinese population, 1987-2015: a systematic review and meta-analysis. Sci Rep 2017; 7: 45000.

[3] Pihlstrom BL, Michalowicz BS and Johnson NW. Periodontal diseases. Lancet 2005; 366: 1809-1820.

[4] Bosshardt DD and Selvig KA. Dental cementum: the dynamic tissue covering of the root. Periodontol 2000 1997; 13: 41-75.

[5] Zeichner-David M. Regeneration of periodontal tissues: cementogenesis revisited. Periodontol 2000 2006; 41: 196-217.

[6] Beertsen W, VandenBos T and Everts V. Root development in mice lacking functional tissue non-specific alkaline phosphatase gene: inhibition of acellular cementum formation. J Dent Res 1999; 78: 1221-1229.

[7] Grzesik WJ and Narayanan AS. Cementum and periodontal wound healing and regeneration. Crit Rev Oral Biol Med 2002; 13: 474-484.
[8] Bosshardt DD. Are cementoblasts a subpopulation of osteoblasts or a unique phenotype? J Dent Res 2005; 84: 390-406.
[9] Cao Z, Zhang H, Zhou X, Han X, Ren Y, Gao T, Xiao Y, de Crombrugghe B, Somerman MJ and Feng JQ. Genetic evidence for the vital function of Osterix in cementogenesis. J Bone Miner Res 2012; 27: 1080-1092.
[10] D'Errico JA, Berry JE, Ouyang H, Strayhorn CL, Windle JJ and Somerman MJ. Employing a transgenic animal model to obtain cementoblasts in vitro. J Periodontol 2000; 71: 63-72.
[11] Kitagawa M, Tahara H, Kitagawa S, Oka H, Kudo Y, Sato S, Ogawa I, Miyaichi M and Takata T. Characterization of established cementoblast-like cell lines from human cementum-lining cells in vitro and in vivo. Bone 2006; 39: 1035-1042.
[12] D'Errico JA, MacNeil RL, Takata T, Berry J, Strayhorn C and Somerman MJ. Expression of bone associated markers by tooth root lining cells, in situ and in vitro. Bone 1997; 20: 117-126.
[13] Santulli G. Angiopoietin-like proteins: a comprehensive look. Front Endocrinol Lausanne 2014; 5: 4.
[14] Kadomatsu T, Endo M, Miyata K and Oike Y. Diverse roles of ANGPTL2 in physiology and pathophysiology. Trends Endocrinol Metab 2014; 25: 245-254.
[15] Kubota Y, Oike Y, Satoh S, Tabata Y, Niikura Y, Morisada T, Akao M, Urano T, Ito Y, Miyamoto T, Nagai N, Koh GY, Watanabe S and Suda T. Cooperative interaction of Angiopoietin-like proteins 1 and 2 in zebrafish vascular development. Proc Natl Acad Sci USA 2005; 102: 13502-13507.
[16] Kitazawa M, Nagano M, Masumoto KH, Shigeyoshi Y, Natsume T and Hashimoto S. Angiopoietin-like 2, a circadian gene, improves type 2 diabetes through potentiation of insulin sensitivity in mice adipocytes. Endocrinology 2011; 152: 2558-2567.
[17] Tabata M, Kadomatsu T, Fukuhara S, Miyata K, Ito Y, Endo M, Urano T, Zhu HJ, Tsukano H, Tazume H, Kaikita K, Miyashita K, Iwawaki T, Shimabukuro M, Sakaguchi K, Ito T, Nakagata N, Yamada T, Katagiri H, Kasuga M, Ando Y, Ogawa H, Mochizuki N, Itoh H, Suda T and Oike Y. Angiopoietin-like protein 2 promotes chronic adipose tissue inflammation and obesity-related systemic insulin resistance. Cell Metab 2009; 10: 178-188.
[18] Morinaga J, Kadomatsu T, Miyata K, Endo M, Terada K, Tian Z, Sugizaki T, Tanigawa H, Zhao J, Zhu S, Sato M, Araki K, Iyama K, Tomita K, Mukoyama M, Tomita K, Kitamura K and Oike Y. Angiopoietin-like protein 2 increases renal fibrosis by accelerating transforming growth factor-beta signaling in chronic kidney disease. Kidney Int 2016; 89: 327-341.
[19] Okada T, Tsukano H, Endo M, Tabata M, Miyata K, Kadomatsu T, Miyashita K, Semba K, Nakamura E, Tsukano M, Mizuta H and Oike Y. Synoviocyte-derived angiopoietin-like protein 2 contributes to synovial chronic inflammation in rheumatoid arthritis. Am J Pathol 2010; 176: 2309-2319.
[20] Horio E, Kadomatsu T, Miyata K, Arai Y, Hosokawa K, Doi Y, Ninomiya T, Horiguchi H, Endo M, Tabata M, Tazume H, Tian Z, Takahashi O, Terada K, Takeya M, Hao H, Hirose N, Minami T, Suda T, Kiyohara Y, Ogawa H, Kaikita K and Oike Y. Role of endothelial cell-derived angptl2 in vascular inflammation leading to endothelial dysfunction and atherosclerosis progression. Arterioscler Thromb Vasc Biol 2014; 34: 790-800.
[21] Ohno T, Yamamoto G, Hayashi JI, Nishida E, Goto H, Sasaki Y, Kikuchi T, Fukuda M, Hasegawa Y, Mogi M, Mitani A. Angiopoietin-like protein 2 regulates Porphyromonas gingivalis lipopolysaccharide-induced inflammatory response in human gingival epithelial cells. PLoS One 2017; 12: e0184825.
[22] Tanoue H, Morinaga J, Yoshizawa T, Yugami M, Itoh H, Nakamura T, Uehara Y, Masuda T, Odagiri H, Sugizaki T, Kadomatsu T, Miyata K, Endo M, Terada K, Ochi H, Takeda S, Yamagata K, Fukuda T, Mizuta H and Oike Y. Angiopoietin-like protein 2 promotes chondrogenic differentiation during bone growth as a cartilage matrix factor. Osteoarthritis Cartilage 2018; 26: 108-117.
[23] Takano A, Fukuda T, Shinjo T, Iwashita M, Matsuzaki E, Yamamichi K, Takeshita M, Sanui T and Nishimura F. Angiopoietin-like protein 2 is a positive regulator of osteoblast differentiation. Metabolism 2017; 69: 157-170.
[24] Wang X, Sun H, Liao H, Wang C, Jiang C, Zhang Y and Cao Z. MicroRNA-155-3p mediates TNF-alpha-inhibited cementoblast differentiation. J Dent Res 2017; 96: 1430-1437.
[25] Hakki SS, Foster BL, Nagatomo KJ, Bozkurt SB, Hakki EE, Somerman MJ and Nohutcu RM. Bone morphogenetic protein-7 enhances cementoblast function in vitro. J Periodontol 2010; 81: 1663-1674.
[26] Saygin NE, Giannobile WV and Somerman MJ. Molecular and cell biology of cementum. Periodontol 2000 2000; 24: 73-98.
[27] Yang LK, Zhu J, Chen YH, Wang DL, Li H, Zhang LJ, Zhou JR and Liu W. Knockdown of angiopoietin-like protein 2 inhibits proliferation and invasion in glioma cells via suppressing the

ERK/MAPK signaling pathway. Oncol Res 2017; 25: 1349-1355.
[28] Umikawa M, Umikawa A, Asato T, Takei K, Matsuzaki G, Kariya K and Zhang CC. Angiopoietin-like protein 2 induces proinflammatory responses in peritoneal cells. Biochem Biophys Res Commun 2015; 467: 235-241.
[29] Odagiri H, Kadomatsu T, Endo M, Masuda T, Morioka MS, Fukuhara S, Miyamoto T, Kobayashi E, Miyata K, Aoi J, Horiguchi H, Nishimura N, Terada K, Yakushiji T, Manabe I, Mochizuki N, Mizuta H and Oike Y. The secreted protein ANGPTL2 promotes metastasis of osteosarcoma cells through integrin alpha5beta1, p38 MAPK, and matrix metalloproteinases. Sci Signal 2014; 7: ra7.
[30] Horiguchi H, Endo M, Kawane K, Kadomatsu T, Terada K, Morinaga J, Araki K, Miyata K and Oike Y. ANGPTL2 expression in the intestinal stem cell niche controls epithelial regeneration and homeostasis. EMBO J 2017; 36: 409-424.
[31] Higuchi C, Myoui A, Hashimoto N, Kuriyama K, Yoshioka K, Yoshikawa H and Itoh K. Continuous inhibition of MAPK signaling promotes the early osteoblastic differentiation and mineralization of the extracellular matrix. J Bone Miner Res 2002; 17: 1785-1794.
[32] Quarto N, Senarath-Yapa K, Renda A and Longaker MT. TWIST1 silencing enhances in vitro and in vivo osteogenic differentiation of human adipose-derived stem cells by triggering activation of BMP-ERK/FGF signaling and TAZ upregulation. Stem Cells 2015; 33: 833-847.
[33] Song F, Sun H, Huang L, Fu D and Huang C. The role of pannexin3-modified human dental pulp-derived mesenchymal stromal cells in repairing rat cranial critical-sized bone defects. Cell Physiol Biochem 2017; 44: 2174-2188.
[34] Yang B, Sun H, Song F, Wu Y and Wang J. Yes-associated protein 1 promotes the differentiation and mineralization of cementoblast. J Cell Physiol 2018; 233: 2213-2224.
[35] Wang C, Liao H, Sun H, Zhang Y and Cao Z. MicroRNA-3064-3p regulates the differentiation of cementoblasts through targeting DKK1. J Periodontal Res 2018; 53: 705-713.
[36] He XX, Guo AY, Xu CR, Chang Y, Xiang GY, Gong J, Dan ZL, Tian DA, Liao JZ and Lin JS. Bioinformatics analysis identifies miR-221 as a core regulator in hepatocellular carcinoma and its silencing suppresses tumor properties. Oncol Rep 2014; 32: 1200-1210.
[37] Zhou J, Wang J, Wu S, Zhu S, Wang S, Zhou H, Tian X, Tang N and Nie S. Angiopoietin-like protein 2 negatively regulated by microRNA-25 contributes to the malignant progression of colorectal cancer. Int J Mol Med 2014; 34: 1286-1292.

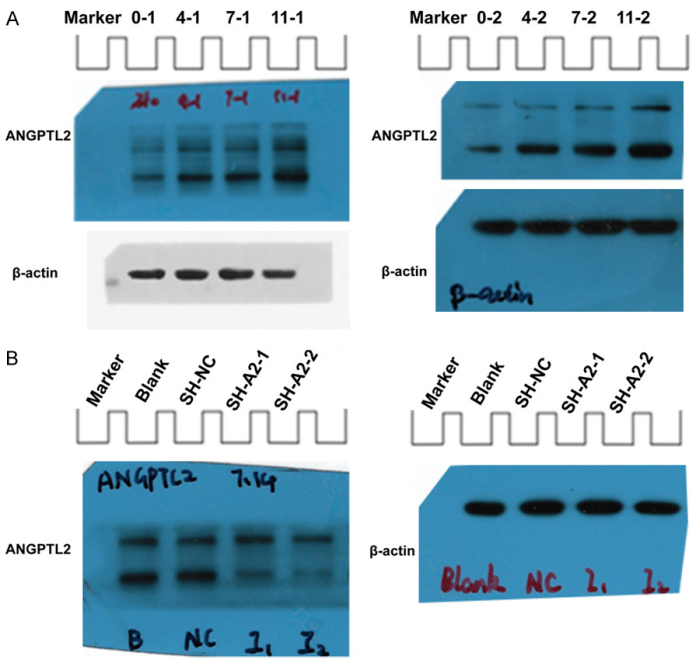

Figure S1. A. OCCM-30 cells were cultured in osteogenic induction medium for 0, 4, 7, and 11 days. The protein samples were collected at the indicated time. B. The protein level of ANGPTL2 was examined after infection of cells with the relevant lentivirus. Each protein was loaded on 10% sodium dodecyl sulfate-polyacrylamide gel electrophoresis (SDS-PAGE) gel and transferred onto a PVDF membrane. The membranes were visualized with an ECL kit (Advansta Inc., Menlo Park, CA, USA) and detected with X-ray films or Odyssey LI-CDR scanner (BD Biosciences, San Jose, CA, USA). β-actin was used as internal control. Notes: Blank, cells without lentivirus infection; SH-NC, SH-NC lentivirus infection; SH-A2, SH-ANGPTL2 lentivirus infection.

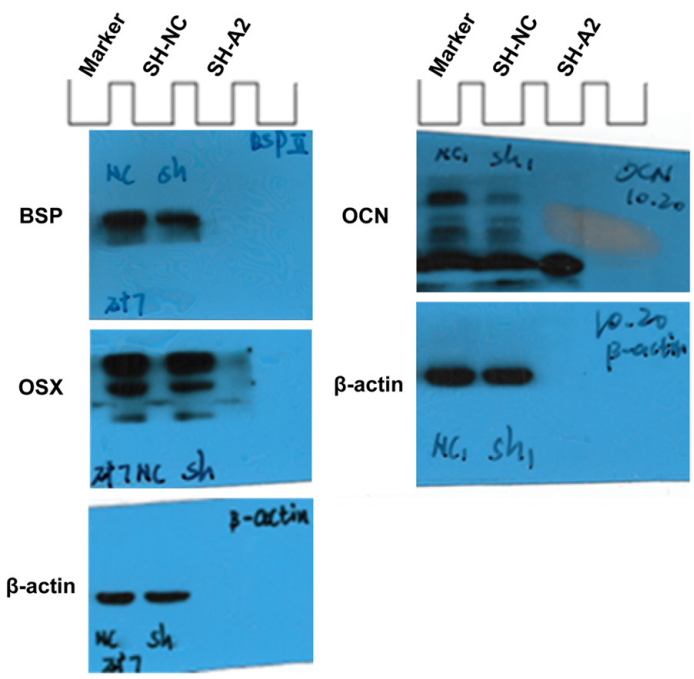

Figure S2. The protein levels of the expression of osterix (OSX), bone sialoprotein (BSP), and osteocalcin (OCN) were detected by Western blotting after osteogenic differentiation of OCCM-30 cells for 7 days. Each protein was loaded onto 10% (for BSP, OSX) or 12% SDS-PAGE (for OCN) gel and transferred onto a PVDF membrane. The membranes were visualized with an ECL kit (Advansta) and detected with X-ray films. β-actin was used as an internal control. Notes: SH-NC, SH-NC lentivirus infection; SH-A2, SH-ANGPTL2 lentivirus infection.

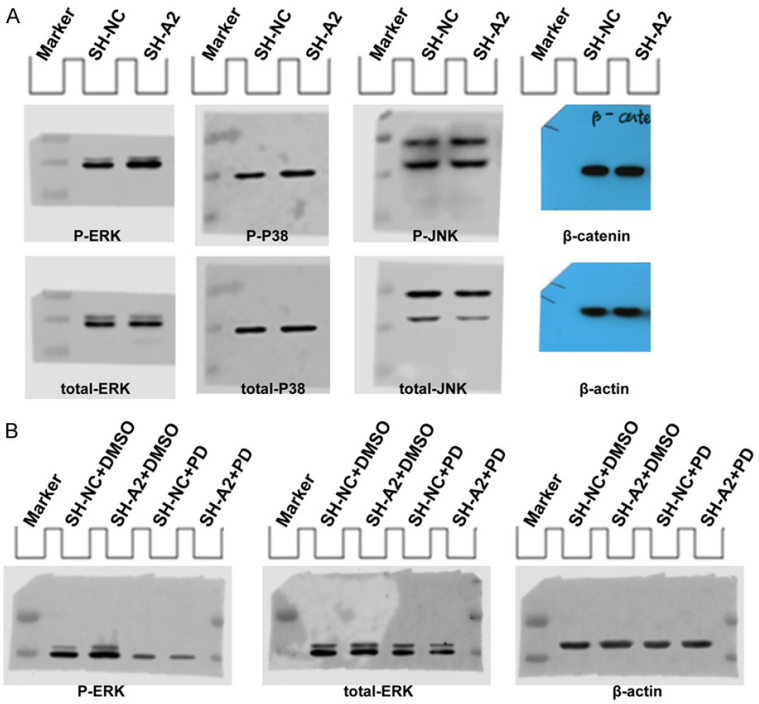

Figure S3. A. After ANGPTL2 inhibition, four different signaling pathways were detected by Western blotting-ERK1/2, P38, JNK, and β-catenin. B. The transfected cells were treated with 10 uM PD98059 in dimethyl sulfoxide (DMSO) or DMSO alone and proteins were collected after 6 h. Each protein was loaded onto 10% SDS-PAGE gel and transferred onto a PVDF membrane. The membranes were visualized with an ECL kit (Advansta) and detected with Odyssey LI-CDR scanner (BD biosciences, USA). Notes: SH-NC, SH-NC lentivirus infection; SH-A2, SH-ANGPTL2 lentivirus infection; DMSO, DMSO treatment; PD, PD98059 treatment.

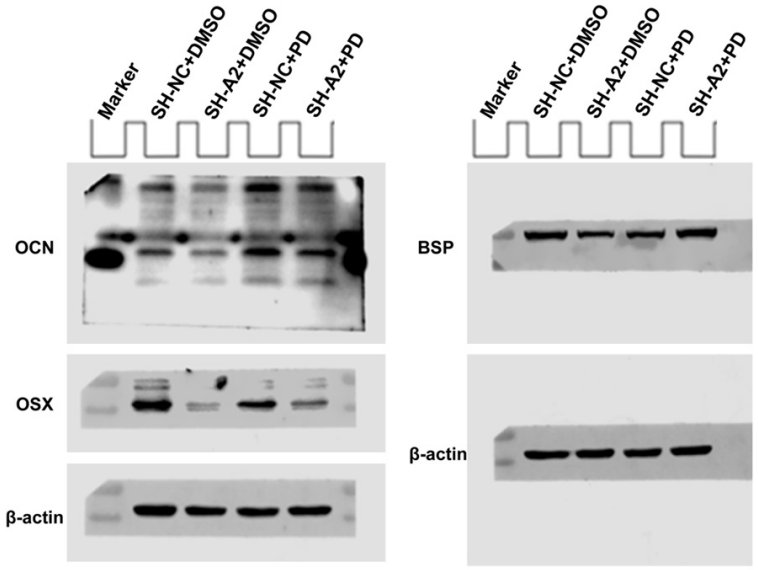

Figure S4. The protein levels of OSX, OCN and BSP were examined by Western blotting on day 7 in SH-NC and SH-ANGPTL2 cementoblast after PD98059 or DMSO treatment. Each protein was loaded onto 10% (for BSP,) or 12% (for OCN and OSX) SDS-PAGE gel and transferred onto a PVDF membrane. The membranes were visualized with an ECL kit (Advansta) and detected with Odyssey LI-CDR scanner (BD biosciences, USA). β-actin was used as the internal control. Notes: SH-NC, SH-NC lentivirus infection; SH-A2, SH-ANGPTL2 lentivirus infection; DMSO, DMSO treatment; PD, PD98059 treatment.